Current Optics and Photonics
Vol. 2, No. 2, April 2018, pp. 125-133

ISSN: 2508-7266(Print) / ISSN: 2508-7274(Online)
DOI: https://doi.org/10.3807/COPP.2018.2.2.125

# Analysis on Design and Fabrication of High-diffraction-efficiency Multilayer Dielectric Gratings

**Hyun-Ju Cho[1]*, Kwang-Hyun Lee[3], Sang-In Kim[2], Jung-Hwan Lee[3], Hyun-Tae Kim[2], Won-Sik Kim[2], Dong Hwan Kim[2], Yong-Soo Lee[2], Seoyoung Kim[4], Tae Young Kim[4], and Chang Kwon Hwangbo[4]****

[1]*Department of Firearms & Optics, Daeduk University, Daejeon 34111, Korea*
[2]*Laser Team, Hanwha Defense Systems, Sungnam 13488, Korea*
[3]*5th R&D Institute, Agency for Defense Development, Daejeon 34186, Korea*
[4]*Department of Physics, Inha University, Inchon 22212, Korea*

(Received November 10, 2017 : revised January 30, 2018 : accepted March 23, 2018)

We report an in-depth analysis of the design and fabrication of multilayer dielectric (MLD) diffraction gratings for spectral beam combining at a wavelength of 1055 nm. The design involves a near-Littrow grating and a modal analysis for high diffraction efficiency. A range of wavelengths, grating periods, and angles of incidence were examined for the near-Littrow grating, for the $0^{th}$ and $-1^{st}$ diffraction orders only. A modal method was then used to investigate the effect of the duty cycle on the effective indices of the grating modes, and the depth of the grating was determined for only the $-1^{st}$-order diffraction. The design parameters of the grating and the matching layer thickness between grating and MLD reflector were refined for high diffraction efficiency, using the finite-difference time-domain (FDTD) method. A high reflector was deposited by electron-beam evaporation, and a grating structure was fabricated by photolithography and reactive-ion etching. The diffraction efficiency and laser-induced damage threshold of the fabricated MLD diffraction gratings were measured, and the diffraction efficiency was compared with the design's value.

*Keywords* : Diffraction grating, Nanostructure fabrication, Multilayer interference coating, Laser damage
*OCIS codes* : (050.1950) Diffraction gratings, (310.1620) Interference coatings, (310.6628) Subwavelength structures, nanostructures, (230.4000) Nanostructure fabrication, (140.3330) Laser damage

## I. INTRODUCTION

The power of fiber lasers has been increasing, and high-power laser systems have been developed by combining the beams of low-power lasers. Coherent beam combining (CBC) and spectral beam combining (SBC) methods are widely used [1]. In the CBC method, the phase of each laser beam must be adjusted coherently for phase matching, by applying a feedback signal to the seed lasers. Thus CBC systems have complicated structures requiring many components. SBC is a simpler method, since a diffraction grating can be used to combine a few laser beams incoherently with slightly different wavelengths, which is also known as wavelength beam combining (WBC) [2-5].

The diffraction grating is one of the key components of an SBC system. Due to ease of fabrication, metals and semiconductors are commonly used to make reflection-type diffraction gratings. Metal gratings such as gold, silver, and aluminum have high reflectance over a broad range of wavelengths, but their laser-induced damage threshold (LIDT) is low, due to the absorption loss of light in the metal. Absorption-free multilayer dielectric (MLD) mirrors are widely used instead of metal reflectors, for their high LIDT and high diffraction efficiency, as shown in Fig. 1.

※The authors contributed equally to this work.
†Corresponding authors: *hjcho@ddc.ac.kr, ORCID 0000-0003-4885-8025
**hwangbo@inha.ac.kr, ORCID 0000-0002-8779-862X

Color versions of one or more of the figures in this paper are available online.

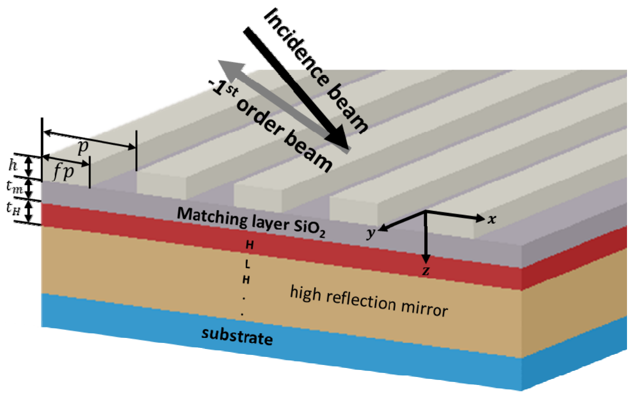


FIG. 1. Schematic diagram of a multilayer dielectric (MLD) diffraction grating. A diffraction grating sits on top of a high MLD reflector, which consists of high- and low-index dielectric layers deposited on a substrate. A matching layer is inserted between them. The grating parameters are the period $p$ of the grating, duty cycle $f$, depth $h$, and matching layer thickness $t$.

A phase diffraction grating is placed on top of an MLD mirror, and a matching layer is inserted between them. The grating's parameters are its period $p$, duty cycle $f$, depth $h$, and matching-layer thickness $t$.

Perry *et al.* were the first to demonstrate an MLD diffraction grating using ZnS and $ThF_4$ for chirped-pulse compression [6]. Frank and Collischon proposed a method using an $MgF_2$ etch-stop layer for perfect etching of an $SiO_2$ top grating [7]. Neauport *et al.* proposed a trapezoid-shaped MLD grating, and achieved 96% diffraction efficiency for a –1$^{st}$-order TE wave at 1053 nm [8]. Martz *et al*. demonstrated a large MLD grating with more than 97% diffraction efficiency across the clear aperture area [9]. Li *et al.* proposed a two-layer trapezoidal grating for a polarization-independent high efficiency MLD grating at the wavelength of a Ti:sapphire laser [10].

The purpose of this study is to design and fabricate a high-diffraction-efficiency MLD grating for spectral beam combination for the wavelengths of a Yb-doped fiber laser. Large angular dispersion is also required to combine many wavelengths in the 1040~1075 nm range from the fiber lasers. In this study, high diffraction efficiency was designed at the –1$^{st}$-order TE wave near the Littrow condition, and compared to the experimental value. To this end in design, the diffraction modes were analyzed by varying the incidence angle and grating line density at a given wavelength, and a modal method was used for the duty cycle and grating depth. The diffraction efficiency was calculated using the finite-difference time-domain (FDTD) method [11, 12]. Two grating designs with different duty cycles were fabricated on top of MLD reflectors, using photolithography and reactive-ion etching. The cross sections were observed using a scanning electron microscope (SEM), the diffraction efficiency was measured, and the laser-induced damage threshold (LIDT) was obtained. The analysis and results in this study could be helpful for various applications, such as unpolarized MLD diffraction gratings with high laser-induced damage, MLD chirped-pulse amplifier gratings, and nanophotonic MLD grating devices.

## II. DESIGN OF MULTILAYER DIELECTRIC GRATINGS

Spectral beam combination of low-power laser beams using a diffraction grating is a simple way of incoherently increasing the power of a laser system. In an SBC system, all the laser beams must be diffracted at a specific diffraction order, then combined to form a high-power laser beam. The combined beam needs to be diffraction limited, as well as having high radiance and high beam quality in the far field. In other words, the diffraction grating for an SBC system should have high diffraction efficiency and high beam quality. Furthermore, if many laser beams over a wide angle of incidence are combined, the angular dispersion should be large. We follow basic principles to design the initial gratings and multilayer dielectric mirrors separately, then refine the parameters of the MLD grating system (grating + matching layer + multilayer mirror) using a matching layer to obtain high diffraction efficiency.

The diffraction-grating equations in reflection ($R$) and transmission ($T$) are

$$\begin{cases} n_i \sin\theta_m = n_i \sin\theta_i + m\dfrac{\lambda}{p} \\ n_s \sin\theta_m = n_i \sin\theta_i + m\dfrac{\lambda}{p} \end{cases} \tag{1}$$

where $p$ is the period of the grating, $n_i$ and $n_s$ are the refractive indices of the incident and transmitted media respectively, $\theta_m$ is the diffraction angle, $\theta_i$ is the angle of incidence, $m$ is the diffraction order, and $\lambda$ is the wavelength of incident light [13, 14]. It is well known that very high diffraction efficiency at the $m^{th}$ order can be obtained from a Littrow grating, which diffracts an incident beam backward toward the source, i.e. $\theta_{-m} = -\theta_i$ [14]. The diffraction efficiency of the –1$^{st}$ order becomes 100% if the Littrow grating for an SBC system diffracts only at the $m$ = –1$^{st}$ order (i.e. Eq. (1) in $R$ mode becomes $\sin\theta_d = \dfrac{\lambda}{2n_i p}$), and if zeroth-order specular reflection is suppressed completely.

The figure of merit for the quality of a Gaussian laser beam is $M^2$, and the combined beam at the Littrow grating can be expressed by

$$M^2 = \sqrt{1 + \left(\frac{\pi w_0 (\Delta\lambda)}{2\lambda p \cos\theta_{-1}}\right)^2}, \tag{2}$$

where $w_0$ is the beam-waist radius of the incident beam, and $\triangle\lambda$ is the bandwidth for a laser beam of wavelength $\lambda$ [3]. High beam quality $(M^2 \approx 1)$ for an SBC beam can be obtained at the Littrow grating if the beam width $(w_0)$, diffraction angle $(\theta_{-1})$, or laser bandwidth $(\triangle\lambda)$ is small, or if the grating period $(p)$ is large.

Hehl *et al.* used the effective index of a diffraction grating to set the range of the grating density, and the incidence angle at which each diffraction mode can exist [15]. Based on their method, Fig. 2 shows the range of diffraction modes as a function of the incidence angle and grating density at a wavelength of 1055 nm, with $n_0 = 1.0$ and $n_s = 1.46$. The $-1^{\text{st}}$ orders in $T$ and $R$ radiate below the lines of $T_{-1}\left(\frac{\lambda}{n_i p} = \sin\theta_i + \frac{n_s}{n_i}\right)$ and $R_{-1}\left(\frac{\lambda}{n_i p} = \sin\theta_i + 1\right)$ respectively. The $+1^{\text{st}}$ and $-2^{\text{nd}}$ orders in $T$ are evanescent above the lines of $T_{+1}\left(\frac{\lambda}{n_i p} = -\sin\theta_i + \frac{n_s}{n_i}\right)$ and $T_{-2}\left(\frac{\lambda}{n_i p} = \frac{1}{2}\sin\theta_i + \frac{n_s}{2n_i}\right)$, respectively. Therefore, the area in red surrounded by the $R_{-1}$, $T_{+1}$, and $T_{-2}$ lines is for only $-1^{\text{st}}$-order diffraction in $R$ and $T$. The Littrow condition at which the $-1^{\text{st}}$ order is diffracted back into the incident direction is shown as a long-dashed line $\left(\frac{\lambda}{n_i p} = 2\sin\theta_i\right)$. Similarly, other specific orders in different colors can be chosen. For example, the blue area is only for the $-1^{\text{st}}$ orders in $R$ and $T$ and the $+1^{\text{st}}$ order in $T$ mode. Figure 2 is very useful for designing a grating of any specific orders in $R$ and $T$.

The angular dispersion of a diffraction grating is given by $D = \frac{d\theta}{d\lambda} = \frac{m}{p\cos\theta_m}$, and the incidence angle at the Littrow condition of $\theta_i = -\theta_{-1}$ can be determined by [16]

$$\theta_i = \tan^{-1}\left(\frac{D\lambda}{2}\right). \tag{3}$$

The period can be determined from the Littrow condition,

$$p = \frac{\lambda}{2n_i \sin\theta_i}. \tag{4}$$

If the angular dispersion of diffraction is $D = 3.5\frac{\text{rad}}{\mu\text{m}}$, the incidence angle from Eq. (3) is $\theta_i \approx 62°$, which is located near the Littrow line in the red area of Fig. 2. The grating period $p$ then becomes 597 nm, according to Eq. (4). This design is shown as a dot, inside the area of the $-1^{\text{st}}$ order in $R$ only and near the Littrow line, in Fig. 2. The period of the fabricated gratings was 575 nm, which is sufficient to achieve the final goal of the SBC system.

The duty cycle $(f)$ and depth $(h)$ of a grating are also important parameters to determine. Clausnitzer *et al.* used a

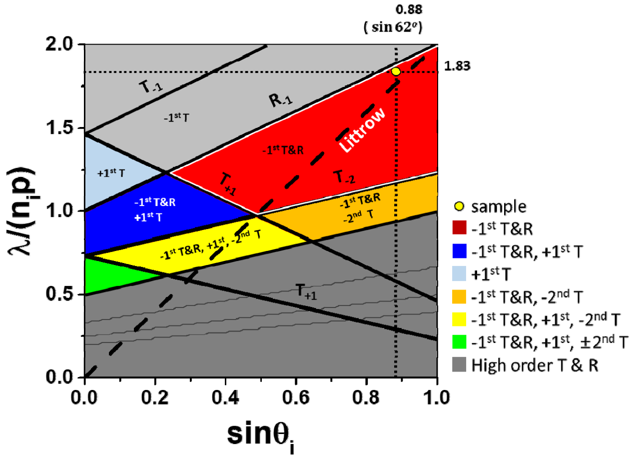


FIG. 2. Dispersion of diffraction orders in reflection and transmission, as a function of incidence angle and (wavelength/grating period). Only the $0^{\text{th}}$ and $-1^{\text{st}}$ orders in $R$ and $T$ exist in an area in red, delimited by $R_{-1}$, $T_{+1}$, and $T_{-2}$ lines. The Littrow condition, at which the $-1^{\text{st}}$ order is diffracted back in the incident direction, is shown as a long-dashed line $\left(\frac{\lambda}{n_i p} = 2\sin\theta_i\right)$. $\lambda$ = 1055 nm, $n_0$ = 1.0 and $n_s$ = 1.46.

simple modal method for estimating the grating efficiency, and showed that the results agree well with those of a rigorous calculation [17]. The dispersion equation of a 1-dimensional periodic diffraction grating with a ridge of thickness $d_r$ and a groove of thickness $d_g$ is:

$$\cos K_{x,in} p = \cos k_{xr} d_r \cos k_{xg} d_g - \Gamma \sin k_{xr} d_r \sin k_{xg} d_g = F(n_e^2) \tag{5}$$

where $K_{x,in} = \frac{\omega}{c} n_i \sin\theta_i$ is the Bloch wave vector in the $x$ direction, $p = d_r + d_g$ is the period of the grating, $f = \frac{d_r}{p}$ is the duty cycle, $k_{xr} = \frac{\omega}{c}\sqrt{n_r^2 - n_e^2}$ and $k_{xg} = \frac{\omega}{c}\sqrt{n_g^2 - n_e^2}$ are respectively the propagation wave vectors in a ridge and groove in the $x$ direction, $n_e$ is the effective index of the grating as a waveguide in the $z$-direction, and $\Gamma$ depends on the polarization: $\Gamma_{TE} = \frac{1}{2}\left(\frac{k_{xr}}{k_{xg}} + \frac{k_{xg}}{k_{xr}}\right)$ for a TE wave, and $\Gamma_{TM} = \frac{1}{2}\left(\frac{n_r^2 k_{xg}}{n_g^2 k_{xr}} + \frac{n_g^2 k_{xr}}{n_r^2 k_{xg}}\right)$ for a TM wave.

An effective index of a propagating mode for transmission in the direction inside the grating can be determined graphically or numerically from Eq. (5), which is a function of $n_e^2$, i.e., $F(n_e^2)$. At the Littrow condition of Eq. (4), the Bloch wave vector is $K_{x,in} = \frac{\omega}{c} n_i \sin\theta_i = \frac{\pi}{p}$ and the left-hand side of Eq. (5) is $\cos K_{x,in} p = -1$. Effective indices of two guided modes for each TE and TM wave are presented as a function of the duty cycle in Fig. 3, in

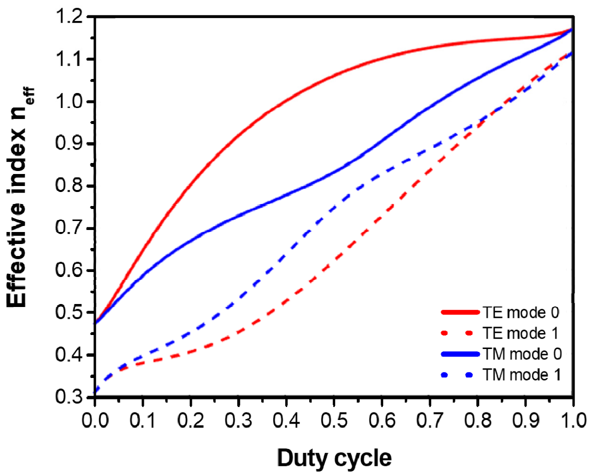


FIG. 3. Effective indices of two guided modes as functions of duty cycle, for TE and TM waves. $p$ = 575 nm, $\lambda$ = 1055 nm, $n_r$ = 1.46, and $n_g$ = 1.0.

which $p = 575$ nm, $\theta_i = 62°$, and $\lambda = 1055$ nm.

The difference in effective indices between $n_{e0}$ and $n_{e1}$ for a TE wave is around 0.5 in $f = 0.3$~0.6, which is much larger than for a TM wave. Two guided modes of $n_{e0}$ and $n_{e1}$ are reflected at a high reflective mirror. If the guided modes interfere constructively to couple completely with only the –1st order diffraction, the diffraction efficiency of the grating at the –1st order for a TE wave is $\eta_{-1} = \sin^2\frac{\triangle\phi}{2}$, where $\triangle\phi = \frac{4\pi}{\lambda}(n_{e0} - n_{e1})h$ is the optical phase thickness. A diffraction efficiency of $\eta_{-1} = 100\%$ can be obtained if the height of the grating is

$$h = \frac{\lambda}{4|n_{e0} - n_{e1}|}. \quad (6)$$

The diffraction grating depth was obtained from Eq. (6) as $h = 538$~643 nm, using the effective refractive indices $f = 0.3$~0.6 in Fig. 3.

In the near-infrared wavelength region, $HfO_2$ and $SiO_2$ are widely used as high ($n = 1.89$) and low ($n = 1.45$) refractive index materials in an MLD mirror, for high LIDT [18, 19]. A 20-layer quarter-wave dielectric reflector was designed and fabricated by electron-beam evaporation. Figure 4 shows the reflectance of both the designed and deposited multilayer dielectric mirrors, at an incidence angle of 62° [20]. The deposited mirror's reflectance for *s*-polarized light is almost 100% around 1055 nm, which matches well with the design.

It was found that the diffraction efficiency for a diffraction grating on top of an MLD mirror system (grating + MLD mirror) was low, due to destructive leaky modes, so a matching layer was inserted between the grating and MLD reflector to obtain high diffraction efficiency, as shown in Fig. 1. In the case of a (grating + matching layer + MLD mirror) system, the design parameters of duty cycle, matching layer thickness, and grating depth obtained using the basic principles above should be optimized further, using an FDTD simulation. The simulations were performed in a duty cycle range of $f = 0.3$~0.7, with matching layer thicknesses of $t_m = 210$~650 nm, and grating depths of $h$ = 210~650 nm.

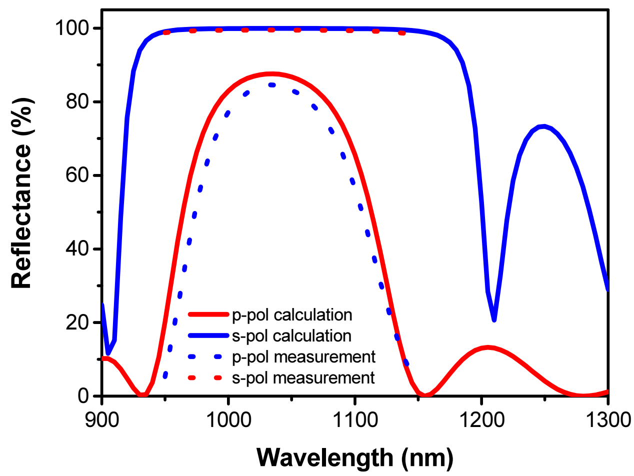


FIG. 4. Reflectance of the calculated and measured MLD mirrors at 62° incidence angle, for *p* and *s* polarizations. $HfO_2$ and $SiO_2$ were used as high- (H) and low- (L) refractive-index materials respectively. Twenty-one quarter-wave H and L layers were deposited.

Figure 5 shows the diffraction efficiency ($\eta_{-1}$) of the –1st-order beam as a function of the grating depth ($h$) and matching layer ($t_m$) at duty cycles of $f = 0.3$, 0.4, 0.5, and 0.6. In the area of high $\eta_{-1}$ (in red), at a given duty cycle the grating depth tends to decrease as the matching layer thickness increases, which may ease fabrication of the grating. As the duty cycle increases, the area of high $\eta_{-1}$ decreases and becomes a thin line, where the matching layer thickness is inversely proportional to the grating thickness. Figure 6 shows $\eta_{-1}$ as a function of the grating depth and duty cycle, at matching layer thicknesses of $t_m = 310$, 410, 510, and 610 nm. The area of high $\eta_{-1}$ increases and shifts to small duty cycle and grating thickness, as the matching layer thickness increases to 510 nm. However, the area decreases at 610 nm and shifts toward a smaller duty cycle and grating thickness.

Based on the FDTD results and for easy fabrication, we set the matching layer thickness as $t_m = 430$ nm and the grating depth as $h = 430$ nm at duty cycles of $f = 0.35$ and 0.5. Figures 7(a) and 7(b) show the calculated diffraction efficiency as a function of wavelength and incidence angle. A duty cycle of $f = 0.35$ exhibits $\eta_{-1} = 94.5\%$ at $\lambda = 1035$ nm and $\theta_i = 62°$, while a duty cycle of the $f = 0.5$ reveals $\eta_{-1} = 98.1\%$ at $\lambda = 1060$ nm and $\theta_i = 62°$. Figure 7(b) shows $\eta_{-1}$ as a function of incidence angle, at $\lambda = 1050$ nm and 1064 nm and $f = 0.35$.

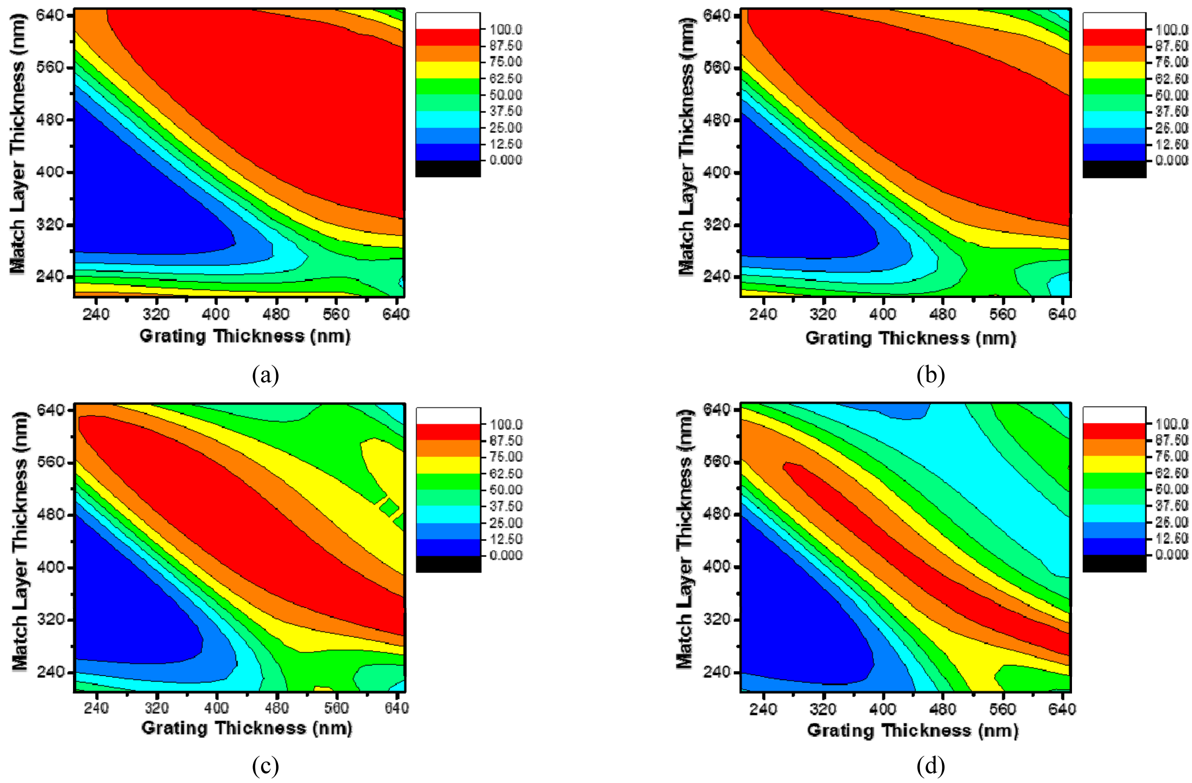


FIG. 5. Calculated $-1^{st}$ diffraction efficiencies as functions of the grating thickness and matching layer thickness, for duty cycles of (a) 0.3, (b) 0.4, (c) 0.5, and (d) 0.6.

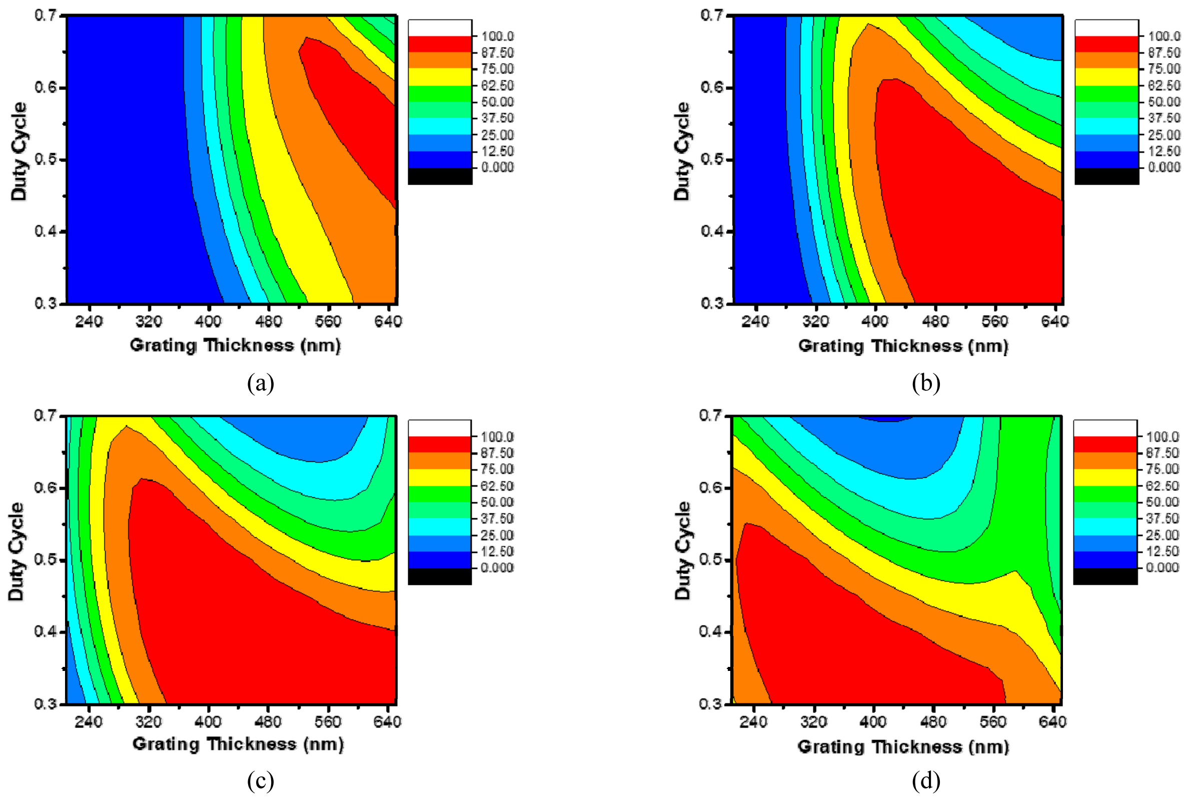


FIG. 6. Calculated $-1^{st}$ diffraction efficiencies as functions of grating thickness and duty cycle, for matching layer thicknesses of (a) 310 nm, (b) 410 nm, (c) 510 nm, and (d) 610 nm.

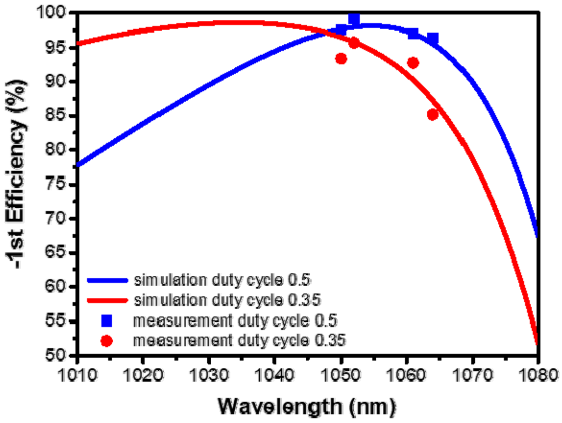


(a)

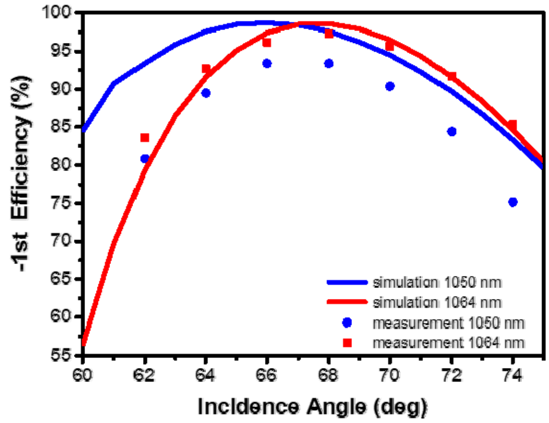


(b)

FIG. 7. (a) Calculated and measured –1st diffraction efficiency of MLD grating as a function of wavelength, for duty cycles of 0.35 and 0.5. (b) Calculated and measured –1st-order diffraction efficiency as a function of incidence angle for duty cycle 0.35, at wavelengths 1050 nm and 1064 nm.

## III. RESULTS AND DISCUSSION

Two types of diffraction gratings were fabricated using photolithography and reactive-ion etching. The gratings had the following characteristics: period $p = 575$ nm, grating depth $h = 430$ nm, and matching layer thickness $t = 430$ nm, with different duty cycles of $f = 0.35$ and 0.5. Two types of Cr photomasks (10 $mm^2$) were fabricated, and a stitching process was used to pattern the binary grating on an MLD mirror coated on Si substrate (50 × 150 mm) using a 1:4 KrF scanner (ASML Co. Ltd.). Grating structures were fabricated by reactive-ion etching (EXELAN HPT, LAM Co. Ltd.) with a gas mixture of $C_4F_8$, $O_2$, and Ar, with 200 W of rf power.

Figure 8 shows SEM images of the fabricated MLD diffraction gratings. The low-magnification SEM images in Figs. 8(a) and 8(c) show the grating ($SiO_2$), matching layer ($SiO_2$), and high index layer ($HfO_2$). The high-magnification images in Figs. 8(b) and 8(d) clearly show the shapes of the diffraction grating. A rectangular MLD grating was formed for the grating with a duty cycle of 0.5, as shown in Fig. 8(d), while a slightly trapezoidal shape was produced for the

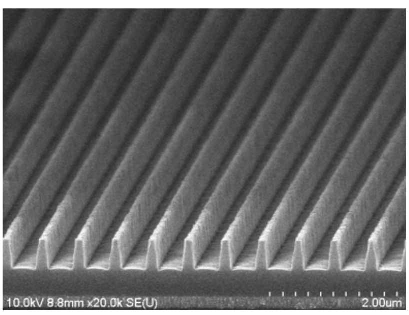


(a)

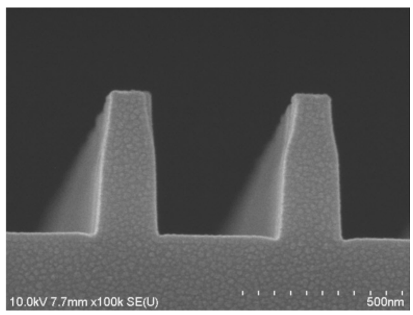


(b)

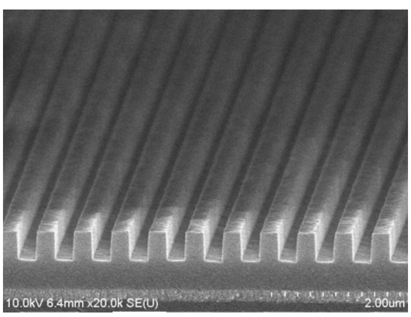


(c)

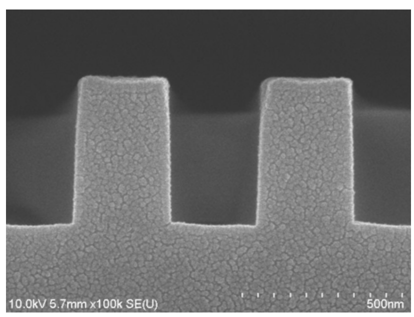


(d)

FIG. 8. SEM images of fabricated MLD gratings. (a) Low and (b) high magnification images, for a duty cycle of 0.35. (c) Low and (d) high magnification images, for a duty cycle of 0.5.

grating with a duty cycle of 0.35, as shown in Fig. 8(b). The performance of the fabricated MLD gratings was measured using in-house equipment, including a 20-mW DFB laser (QLD1061-5330, QD Laser) with wavelengths of 1050 nm, 1052 nm, 1061 nm, and 1064 nm, and a thermal infrared power detector (CLD 1015, Thorlab). Measured diffraction efficiency at four wavelengths is shown in Fig. 7(a), along with the simulations. The maximum efficiency for the duty cycle 0.35 MLD grating was 95.7% at 1052 nm, and that for the duty cycle 0.5 was 99.1% at the same wavelength. It is noted that the measured diffraction efficiencies at four wavelengths for both MLD gratings are quite close to the simulated curves. Figure 7(b) shows the diffraction efficiency as a function of incidence angle, for duty cycle 0.35. The measured maximum efficiency at 1050 nm was 93.4% at an incidence angle of 66°, while the maximum efficiency at 1064 nm was 96.2% at 68°. It is noted that the measured diffraction efficiency at 1064 nm is quite close to the simulated curve, while that at 1050 nm shows a slight difference between the two. The discrepancy in diffraction efficiency between simulation and measurement might have come from alignment error in the measurement system, or instability of the detector or light source.

The laser-induced damage threshold of the fabricated MLD gratings was measured using a cw laser (1 kW output power, IMPAC IN5, Lumasense Inc.) with a beam diameter of 5.85 mm at the MLD grating. The surface of the MLD grating was irradiated by the laser beam and observed by a CCD camera. Temperature variation of the surface was measured by a pyrometer (IMPAC IN5, Lumasense Inc.). As shown in Fig. 9, the surface temperature gradually increased with increasing irradiation time, and the temperature change was larger when the power of the laser was higher. The maximum temperature for the duty cycle 0.35 MLD grating increased up to 45°C during 55 seconds of laser irradiation time, while the temperature for duty cycle 0.5 was up to 55°C. No visual damage was found in the

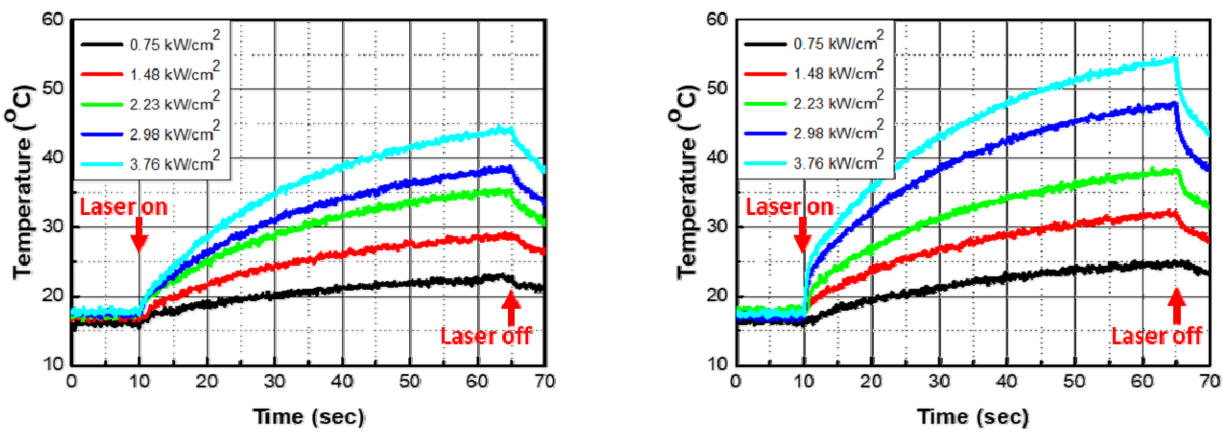


(a) (b)

FIG. 9. Measured surface temperature of MLD grating as a function of laser irradiation time: (a) duty cycle 0.35, (b) duty cycle 0.5.

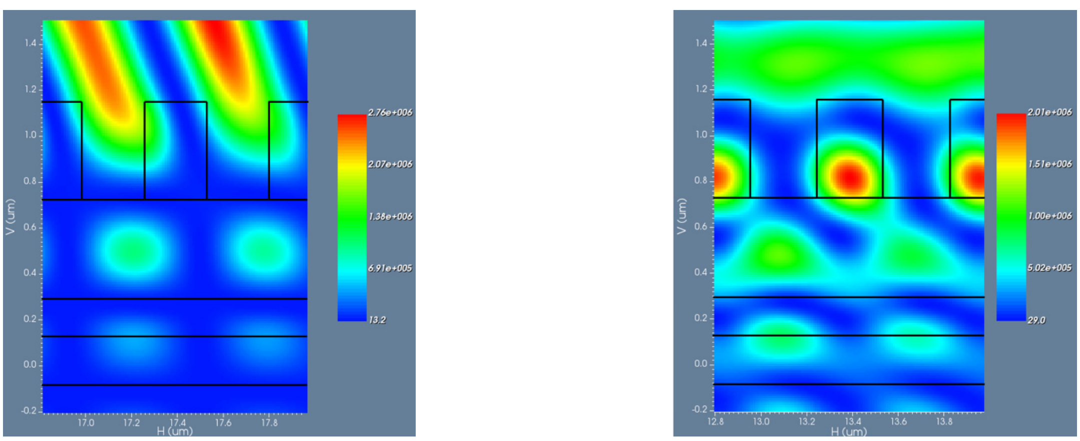

(a) (b)

FIG. 10. Electric-field intensity distribution of MLD grating for a duty cycle of 0.5, at (a) $\theta_i = 62°$ and $\eta_{-1} = 98.1\%$, and (b) $\theta_i = 31°$ and $\eta_{-1} = 0\%$.

CCD camera, and, furthermore, no trace of laser damage was observed upon optical-microscope inspection at the maximum laser power irradiation of 3.76 kW/cm$^2$. It seems that the LDIT of the fabricated MLD grating was greater than 3.76 kW/cm$^2$, which was the maximum, due to the limit of the laser's power and the focal length of the focusing lens.

The electric field intensity distribution of the diffraction grating was investigated, to identify the diffraction efficiency and the LIDT of the MLD gratings. Figure 10(a) shows the intensity distribution of the grating with $f = 0.5$ at $\theta_i =$ 62° with high diffraction efficiency. The $-1^{st}$-order diffracted beam with well-aligned wavefronts propagates backward compared to the incident wave's direction, which indicates that the grating modes are constructively interfering within the grating, and are coupled to the $-1^{st}$-order diffraction beam. A strong intensity distribution is not present at the edge or interface of the diffraction grating, and exists outside of the grating structure, which implies that the LIDT could be high.

Figure 10(b) shows the electric-field intensity distribution of the grating with $f = 0.5$ at $\theta_i = 30°$ with low $-1^{st}$ diffraction efficiency. The diffracted intensity is very low in the incident medium, and the wavefronts are not observed, which indicates low diffraction efficiency. There is high intensity in the ridge of the grating, which could result in low LIDT. This figure agrees well with the result from Neauport *et al.*, in that the presence of high intensity within the grating reduces the LIDT of the MLD grating [8].

## IV. CONCLUSION

This study analyzed the design and fabrication of high-diffraction-efficiency MLD diffraction gratings for spectral beam combining of Yb-doped fiber laser wavelengths. We reported basic design steps and a modal analysis for a near-Littrow grating with high diffraction efficiency. We found a range of grating densities at a wavelength of 1055 nm and incidence angles that allow only the $0^{th}$ and $-1^{st}$ orders of diffraction in the reflection. Two effective indices of the grating modes were calculated as a function of the duty cycle, from the dispersion equation of the Littrow grating. The maximum-interference condition coupled with $-1^{st}$-order diffraction was used to determine the range of duty cycle and grating depth. Finally, an FDTD simulation was used to obtain optimized design parameters for the grating and the matching layer, for high diffraction efficiency.

Two MLD gratings with the same grating parameters and matching layer thickness were fabricated, at different duty cycles of 0.35 and 0.5. The SEM images clearly showed the cross sections of the grating and MLD reflector. The diffraction efficiency and LIDT of each fabricated MLD diffraction grating were measured, and the diffraction efficiency was compared to the designed value. The analysis and results in this study could be helpful for the design and fabrication of MLD diffraction gratings for polarization control and high laser-induced damage, MLD chirped-pulse amplifier gratings, and nanophotonic MLD grating devices.

## ACKNOWLEDGEMENT

This research was supported by Hanwha Defense Systems, and we thank them for their financial support. C.K.H. acknowledges the support from the Inha University Research Grant and the Basic Science Research Program through National Research Foundation (NRF) of Korea (NRF-2016 R1D1A1A09919495).

## REFERENCES

1. T. Y. Fan, "Laser beam combining for high-power, high-radiance source," IEEE J. Sel. Topics Quantum Electron. **11**, 567 (2005).
2. C. Wirth, O. Schmidt, I. Tsybin, T. Schreiber, T. Peschel, F. Bruckner, T. Clausnitzer, J. Limpert, R. Eberhardt, A. Tunnermann, M. Gowin, E. Have, K Ludewigh, and M. Jung, "2 kW incoherent beam combining of four narrow linewidth photonic crystal fiber amplifiers," Opt. Express **17**, 1178 (2009).
3. T. H. Loftus, A. M. Thomas, P. R. Hofman, M. Norsen, R. Royse, A. Liu, and E. C. Honea, "Spectrally beam-combined fiber lasers for high-average-power applications," IEEE J. Quantum Electron. **13**, 487 (2007).
4. S. A. Kemme, D. A. Scrymgeour, and D. W. Peters, "High efficiency diffractive optical elements for spectral beam combining," SPIE **8381**, 83810Q (2014).
5. M. Heon, Y. Jung, J. Park, H. Jeong, J. Kim, and H. Seo, "High-power Quasi-continuous wave operation of incoherently combined Yb-doped fiber lasers" Curr. Opt. Photon. **1**, 525 (2017).
6. M. D. Perry, R. D. Boyd, J. A. Britten, D. Decker, and B. W. Shore, "High-efficiency multilayer dielectric diffraction gratings," Opt. Lett. **21**, 940 (1995).
7. M. Frank and M. Colloschon, "Dielectric multilayer grating designs with maximum diffraction efficiencies," Opt. Eng. **37**, 1696 (1998).
8. J. Neauport, E. Lavastre, G. Raze, G. Dupuy, N. Bonod, M. Balas, G. Villele, J. Flamand, S. Kaladgew, and F. Fesserouer, "Effect of electric field on laser induced damage threshold of multilayer dielectric gratings," Opt. Express **15**, 12508 (2007).
9. D. H. Martz, H. Y. Nguyen, D. Patel, J. A. Britten, D. Alessi, E. Krous, Y. Wang, M. A. Larotonda, J. George, B. Knollenberg, B. M. Luther, J. J. Rocca, and C. S. Menoni, "Large area high efficiency broad bandwidth 800 nm dielectric gratings for high energy laser pulse compression," Opt. Express **17**, 23809 (2009).
10. L. Li, Q. Liu, J. Chen, L. Wang, Y. Jin, Y. Yang, and J. Shao, "Polarization-independent broadband dielectric bilayer gratings for spectral beam combining system," Opt. Commun. **385**, 97 (2017).

11. OptiFDTD simulation software (https://optiwave.com/optifdtd-overview/).
12. D. M. Sullivan, *Electromagnetic simulation using the FDTD method* (IEEE Press, 2000).
13. E. Hecht, "Optics," 4th ed. (Addison Wesley Longman, 2002), pp. 478-481.
14. E. G. Loewen and E. Popov, *Diffraction gratings and applications* (Marcel Decker, New York, 1997), pp. 44-46, 375-376.
15. K. Hehl, J. Brischoff, U. Mohaupt, M. Palme, B. Schnabel, L. Wenke, R. Bodefeld, W. Theobald, E. Welsch, R. Sauerbrey, and H. Heyer, "High-efficiency dielectric reflection gratings: design, fabrication, and analysis," Appl. Opt. **38**, 6257 (1999).
16. A. Sanchez-Rubio, T. Y. Fan, S. J. Augst, A. K. Goyal, K. J. Creedon, J. T. Gopinath, V. Daneu, B. Chann, and R. Huang, "Wavelength beam combining for power and brightness scaling of laser systems," Lincoln Lab J. **20**, 52 (2014).
17. T. Clausnitzer, T. Kampfe, E. Kely, and A. Tunnermann, "An intelligible explanation of highly-efficient diffraction in deep dielectric rectangular transmission gratings," Opt. Express **13**, 10448 (2005).
18. C.J. Stolz, "1064-nm Fabry-Perot transmission filter laser damage competition," SPIE **9237**, 92370N (2014).
19. L. Gallais, B. Mangote, M. Zerrad, M. Commandre, A. Melninkaitis, J. Mirauskas, M. Jeskevic, V. Sirutkaitis, "Laser induced damage of hafnia coatings as a function of pulse duration in the femtosecond to nanosecond range," Appl. Opt. **50**, C178 (2011).
20. Essential Macleod thin film software (Thin Film Center Inc, Tucson, AZ, USA).